Published by Nigerian Society of Physical Sciences. Hosted by FLAYOO Publishing House LTD

Recent Advances in Natural Sciences

Journal Homepage: https://flayoophl.com/journals/index.php/rans

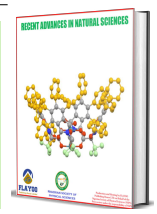

Solving hyperchaotic initial value problems using second derivative extended trapezoidal rule of the second kind blended with generalized backward differentiation formulae with variable step size

E. J. Onoja*, U. W. Sirisena

[a]*Department of Mathematics, University of Jos. P.M.B 2084, Jos-Plateau State, Nigeria*

ARTICLE INFO

Article history:
Received: 05 March 2024
Received in revised form: 24 July 2024
Accepted: 01 August 2024
Available online: 24 August 2024

Keywords: SDBETR$_2$s blended with GBDF, Variable stepsize, Hyperchaotic IVPs

DOI:10.61298/rans.2024.2.2.86

ABSTRACT

This paper aims to evaluate the accuracy and performance of the second derivative block extended trapezoidal rule of the second kind, blended with generalized backward differentiation formulae using variable step sizes, in solving hyperchaotic initial value problems. Hyperchaotic systems, known for their rapidly changing solutions and extreme sensitivity to initial conditions, pose significant challenges for numerical methods. Traditional approaches often involve linearizing the systems or solving them in multiple sub-intervals, followed by combining the results. However, these methods can introduce errors due to the subdivision of intervals. The proposed method, which integrates the second derivative block extended trapezoidal rule with generalized backward differentiation formulae, offers a more precise solution by eliminating the need for interval subdivision and direct linearization. The continuous formulation of this method is derived using a multistep inversion technique that blends two linear multistep methods, while the discrete schemes are deduced from their continuous interpolants. Convergence analyses of these schemes are presented, demonstrating the efficiency and accuracy of the proposed block methods. As a result, these methods are well-suited for solving hyperchaotic and other nonlinear ordinary differential equations.

1. INTRODUCTION

Hyperchaotic systems are chaotic systems that have complex nonlinear dynamics which are also sensitive to initial conditions. Lyapunov exponent measures the rate of divergence or convergence along one axe in the phase space. A positive Lyapunov exponent indicates chaotic system. A hyperchaotic system is a chaotic system with at least two positive Lyapunov exponents. Rosseler was the first to introduce hyperchaotic ordinary differential equations (ODEs) in his work on chemical reactions Ref. [1]. Since then, there have been many new hyperchaotic systems, like the Qi system, the Chen system, the Chua system, and so on. Hyperchaotic systems have a complex nonlinear nature; they have high capacity, security, and efficiency, and they have applications in several areas, including electronic oscillators, encryption, and secure communication. The most commonly used method for solving hyperchaotic systems is analytical methods Refs. [2, 3], which involve linearization of the differential equa-

*Corresponding Author Tel. No.: +234-803-9401-938.
e-mail: Janet4christ35@gmail.com (E. J. Onoja)

tions with slow convergence. Also, the semi-analytical method involves splitting large intervals into smaller sub-intervals, solving hyperchaotic systems on a sequence of intervals and joining the resulting solutions at the end of the interval. This form introduces errors and is time-consuming because of the many smaller intervals. Furthermore, Refs. [4, 5] used the semi-analytical methods, which are based on the spectral method, to solve hyperchaotic systems. This paper is concerned with constructing second derivative block extended trapezoidal rule of the second kind blended with the backward differentiation formulae with better accuracy and stability properties. Consider hyperchaotic system of the initial value problem, defined as:

$$y'(x) = f(x, y(x)), y(x_0) = y_0, \tag{1}$$

on the interval $I = [x_0, x_N]$, where $y : [x_0, x_N] \rightarrow \Re^m$ and $f : [x_0, x_N] \rightarrow \Re^m \times \Re^m$ is continuous, and differentiable. This research is concerned with finding the numerical solutions of equation (1) using second derivative methods. The first section has the introduction, and the second section is the derivation techniques. The third section includes the convergence and stability analysis of the methods, while the last section tests the robustness of these new methods by solving some real-life hyperchaotic ODEs.

1.1. THEOREM (EXISTENCE AND UNIQUENESS OF SOLUTIONS)

Let f(x, y) be defined and continuous for all points (x, y) in an open region of two-dimensional real Euclidean space D, defined by $a \leq x \leq b, -\infty<y<\infty$,a and b finite, and let there exist a constant L such that, for every (x, y) and$(x, y*)$ are both in D, $|f(x, y) - f(x, y*)| \leq L|y - y*|$. Then, if y_0 is any given number, there exist a unique solution y(x) of the IVP Eq. (1), where y(x) is continuous and differentiable for all (x, y) in D.

2. DERIVATION TECHNIQUES

2.1. THE SECOND DERIVATIVE MULTISTEP COLLOCATION METHOD

The method carried described in Ref. [6], will be used in this derivation, to construct a k-step second derivative multistep collocation method as:

$$y(x) = \sum_{j=0}^{t-1} \alpha_j(x) y_{n+j} + h_n \sum_{j=0}^{m-1} \beta_j(x) f_{n+j} + h_n^2 \sum_{j=0}^{m-1} \lambda_j(x) y''_{n+j}, \tag{2}$$

where h_n is the variable step size, $\alpha_j(x), \beta_j(x)$,and $\lambda_j(x)$are the continuous coefficients of the method defined as;

$$\alpha_j(\overline{x}) = \sum_{i=0}^{t+m-1} \alpha_{j,i+1} x^i, j \in \{0, ..., t-1\}$$

$$\beta_j(\overline{x}) = \sum_{i=0}^{t+m-1} \beta_{j,i+1} x^i, j \in \{0, ..., m-1\}$$

$$\lambda_j(\overline{x}) = \sum_{i=0}^{t+m-1} \lambda_{j,i+1} x^i, j \in \{0, ..., m-1\}. \tag{3}$$

Table 1. Comparison between SDETR$_2$s blended with GBDF k = 3, 5 and MSRM using Problem 1 with h=10^{-1} to 10^{-5}.

t	SDETR$_2$s with GBDF k= 3	SDETR$_2$s with GBDF k= 5	MSRM
y1(t)			
2	-2.91138	-2.91138	-2.91138
4	-3.63001	-3.63001	-3.63001
6	2.80571	2.80571	2.80571
8	0.01134	0.01134	0.01134
10	-0.80219	-0.80219	-0.80219
y2(t)			
2	21.73155	21.73155	21.73155
4	6.52144	6.52144	6.52144
6	-2.77638	-2.77638	-2.77638
8	2.09585	2.09585	2.09585
10	16.48559	16.48559	16.48559
y3(t)			
2	-3.24491	-3.24491	-3.24491
4	-6.30881	-6.30881	-6.30881
6	-2.37099	-2.37099	-2.37099
8	-0.14880	-0.14880	-0.14880
10	-0.06690	-0.06690	-0.06690
y4(t)			
2	23.96851	23.96851	23.96851
4	11.30830	11.30830	11.30830
6	4.65208	4.65208	4.65208
8	-4.99685	-4.99685	-4.99685
10	1.98179	1.98179	1.98179
y5(t)			
2	44.32071	44.32071	44.32071
4	14.68007	14.68007	14.68007
6	39.34559	39.34559	39.34559
8	33.79560	33.79560	33.79560
10	50.59739	50.59739	50.59739
y6(t)			
2	26.54682	26.54682	26.54682
4	3.25221	3.25221	3.25221
6	12.99055	12.99055	12.99055
8	8.02232	8.02232	8.02232
10	24.48234	24.48234	24.48234

To determine the continuous coefficients $\alpha_j(x), \beta_j(x)$, and $\lambda_j(x)$ the following conditions are imposed:

$$\alpha_j(\overline{x}_{n+1}) = \delta_{ij}, j = 0, ..., t-1; i = 0, ..., t-1$$

$$h_n \beta_j(\overline{x}_{n+1}) = 0, j = 0, ..., m-1; i = 0, ..., t-1 \tag{4}$$

$$h_n^2 \lambda_j(\overline{x}_{n+1}) = 0, j = 0, ..., m-1; i = 0, 1, ..., t-1,$$

$$\alpha'_j(\overline{x}_i) = 0, j = 0, ..., t-1; i = 0, ..., m-1$$

$$h_n \beta'_j(\overline{x}_i) = \delta_{ij}, j = 0, ..., m-1; i = 0, ..., m-1 \tag{5}$$

$$h_n^2 \lambda'_j(\overline{x}_i) = 0, j = 0, ..., m-1; i = 0, 1, ..., m-1,$$

Table 2. Comparison between SDETR$_2$s blended with GBDF k=5 and MSRM using Problem 2 with h=10^{-1} to 10^{-5}.

	t	SDETR$_2$s with GBDF k= 3	SDETR$_2$s with GBDF k= 5	MSRM
y1(t)				
	3	-3.85711	-3.85711	-3.85711
	10	-0.33729	-0.33729	-0.33729
	17	0.12630	0.12630	0.12630
	24	0.05091	0.05091	0.05091
	31	-2.55034	-2.55034	-2.55034
	38	-3.93154	-3.93154	-3.93154
y2(t)				
	3	-5.66683	-5.66683	-5.66683
	10	-0.49554	-0.49554	-0.49554
	17	0.18555	0.18555	0.18555
	24	0.07480	0.07480	0.07480
	31	-3.74694	-3.74694	-3.74694
	38	-5.77619	-5.77619	-5.77619
y3(t)				
	3	-5.20445	-5.20445	-5.20445
	10	-0.49104	-0.49104	-0.49104
	17	0.15550	0.15550	0.15550
	24	0.19500	0.19500	0.19500
	31	-0.79819	-0.79819	-0.79819
	38	-5.33693	-5.33693	-5.33693
y4(t)				
	3	-7.64635	-7.64635	-7.64635
	10	-0.72144	-0.72144	-0.72144
	17	0.22846	0.22846	0.22846
	24	0.28649	0.28649	0.28649
	31	-1.17270	-1.17270	-1.17270
	38	-7.84098	-7.84098	-7.84098
y5(t)				
	3	15.05932	15.05932	15.05932
	10	10.73663	10.73663	10.73663
	17	14.25582	14.25582	14.25582
	24	19.33844	19.33844	19.33844
	31	25.34856	25.34856	25.34856
	38	14.98250	14.98250	14.98250

It follows from equation (7) the columns of C = D^{-1}, give the elements of the continuous coefficients $\alpha_j(x), \beta_j(x)$, and $\lambda_j(x)$ of the continuous scheme (Equation 3).

and

$$\begin{aligned} &\alpha_j''(\overline{x}_i) = 0, j = 0, ..., t-1; i = 0, ..., m-1 \\ &h_n\beta_j''(\overline{x}_i) = 0, j = 0, ..., m-1; i = 0, ..., m-1 \\ &h_n^2\lambda_j''(\overline{x}_i) = \delta_{ij}, j = 0, ..., m-1; i = 0, 1, ..., m-1, \end{aligned} \tag{6}$$

where $\overline{x}_j$, j = 0, 1, …, m-1 are the m distinct collocation points used and t, 0<$t \leq k$ the number of interpolation points and equation (4) – (5) can be written in matrix form as:

$$DC = 1, \tag{7}$$

where I is the identity matrix of dimension $(t+m)\times(t+m)$ while D and $C$are matrices defined as:

$$D = \begin{pmatrix} 1 & x_n & x_n^2 & ... & x_n^{t+m-1} \\ 1 & x_{n+1} & x_{n+1}^2 & ... & x_{n+1}^{t+m-1} \\ \vdots & \vdots & \vdots & ... & \vdots \\ 1 & x_{n+t-1} & x_{n+t-1}^2 & ... & x_{n+t-1}^{t+m-1} \\ 0 & 1 & 2\overline{x_0} & ... & (t+m-1)x_0^{t+m-2} \\ \vdots & \vdots & \vdots & ... & \vdots \\ 0 & 1 & 2\overline{x_{m-1}} & ... & (t+m-1)\overline{x_{m-1}^{t+m-2}} \\ 0 & 0 & 2 & ... & (t+m-2)(t+m-1)\overline{x_0^{t+m-3}} \\ \vdots & \vdots & \vdots & ... & \vdots \\ 0 & 0 & 2 & ... & (t+m-2)(t+m-1)\overline{x_{m-1}^{t+m-3}}, \end{pmatrix} \tag{8}$$

$$C = \begin{pmatrix} \alpha_{0,1} & \alpha_{1,1} & ... & \alpha_{t-1,1} & h_n\beta_{0,1} & ... & h_n\beta_{m-1,1} & h_n^2\lambda_{0,1} & ... & h_n^2\lambda_{m-1,1} \\ \alpha_{0,2} & \alpha_{1,2} & ... & \alpha_{t-1,2} & h_n\beta_{0,2} & ... & h_n\beta_{m-1,2} & h_n^2\lambda_{0,2} & ... & h_n^2\lambda_{m-1,2} \\ \vdots & \vdots & ... & \vdots & \vdots & ... & \vdots & \vdots & ... & \vdots \\ \alpha_{0,t+m} & \alpha_{1,t+m} & ... & \alpha_{t-1,t+m} & h_n\beta_{0,t+m} & ... & h_n\beta_{m-1,t+m} & h_n^2\lambda_{m-1,t+m} & ... & h_n^2\lambda_{m-1,t+m}. \end{pmatrix} \tag{9}$$

2.2. DERIVATION OF CONTINUOUS SECOND DERIVATIVE CONVENTIONAL FORMS OF EXTENDED TRAPEZOIDAL RULES OF THE SECOND KIND BLENDED WITH GENERALIZED BACKWARD DIFFERENTIATION FORMULAE (SDETR$_2$S BLENDED WITH GBDF) FOR K = 3 AND 5

As defined in Refs. [6, 7], a second derivative ETR$_2$s blended with GBDF is defined as:

$$y(x) = \sum_{j=0}^{k-1} \alpha_j(x)y_{n+j} + h_n[\beta_v(x)f_{n+v-1} + \beta_v(x)f_{n+v}] + h_n^2\lambda_u(x)g_{n+u}, \tag{10}$$

Table 3. Comparison between SDETR$_2$s blended with GBDF k=3, 5 with $h = 10^{-1} to 10^{-5}$ and ODE 45 using Problem 3.

	t	SDETR$_2$s with GBDF k= 3	SDETR$_2$s with GBDF k= 5	ODE 45
y1(t)				
	2	-5.746066	-5.746066	-5.746695
	4	0.704068	0.704068	0.703867
	6	4.772807	4.772807	4.772186
	8	-1.656413	-1.656413	-1.656500
	10	1.421949	1.421949	1.421949
y2(t)				
	2	-0.686392	-0.686392	-0.686321
	4	0.251313	0.251313	0.251329
	6	1.608418	1.608418	1.608104
	8	-0.273639	-0.273639	-0.273534
	10	0.817538	0.817538	0.817270
y3(t)				
	2	4.752034	4.752034	4.752228
	4	4.091915	4.091915	4.092114
	6	3.071328	3.071328	3.071401
	8	4.143334	4.143334	4.143532
	10	2.578950	2.578950	2.579065
y4(t)				
	2	0.586958	0.586958	0.586801
	4	-5.1664589	-5.1664589	-5.166404
	6	-16.184737	-16.184737	-16.184383
	8	-3.211817	-3.211817	-3.211877
	10	8.694178	8.694178	8.694357

where,

$$v = \left[\left[\frac{k+1}{2}\right]\right], \; and \; [[]], \tag{11}$$

is the greatest integer function.

CASE k =3: Letting v = u = 2 and equation (10) becomes;

$$y(x) = \alpha_0(x)y_n + \alpha_1(x)y_{n+1} + h_n[\beta_1(x)f_{n+1} + \beta_2(x)f_{n+2}] + h_n^2\lambda_2(x)g_{n+2}. \tag{12}$$

Computing the inverse of the D matrix obtained from equation (12) using Maple 18 and from equation 4 to 6 we obtain the continuous coefficients with $\eta = (x - x_n)$ as follows:

$$\alpha_0(\eta+x_n) = \frac{1}{8h_n^4}[\eta^4 - 7h_n\eta^3 + 18h_n^2\eta^2 - 20h_n^3\eta + 8h_n^4]$$

$$\alpha_1(\eta+x_n) = \frac{1}{h_n^4}[-\eta^4 + 6h_n\eta^3 - 12h_n^2\eta^2 + 8h_n^3\eta - 8h_n^4]$$

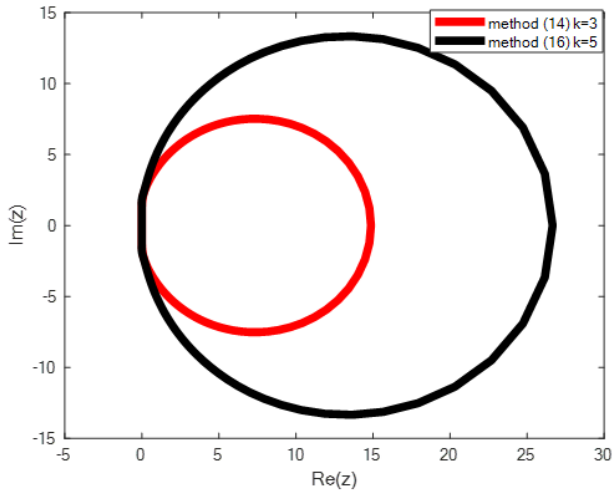

Figure 1. The region of absolute stability of the methods in Eq. (14) and Eq. (16).

$$\beta_1(\eta+x_n) = \frac{1}{4h_n^4}[7\eta^4 - 41h_n\eta^3 + 78h_n^2\eta^2 - 44h_n^3\eta - 44h_n^4]$$

$$\beta_2(\eta+x_n) = \frac{1}{4h_n^3}[-3\eta^4 + 17\eta^3 - 30h_n\eta^2 + 16h_n^2\eta - 16h_n^3]. \tag{13}$$

The continuous scheme is evaluated at $\eta = 3h_n$ and its first derivative at $\eta = (0, 3h_n)$ to have the following three discrete schemes.

$$y_{n+1} = \frac{5}{28}h_n^2g_{n+2} - \frac{1}{56}h_nf_{n+3} - \frac{9}{14}h_nf_{n+2} - \frac{23}{56}h_nf_{n+1} + \frac{29}{28}y_{n+2} - \frac{1}{28}y_n$$

$$y_{n+2} = -\frac{2}{23}h_n^2g_{n+2} + \frac{12}{23}h_nf_{n+2} + \frac{16}{23}h_nf_{n+1} + \frac{2}{23}h_nf_n + \frac{16}{23}y_{n+1} + \frac{7}{23}y_n$$

$$y_{n+3} = 3h_n^2g_{n+2} - 9h_nf_{n+2} - 6h_nf_{n+1} + \frac{33}{2}h_nf_{n+1} + \frac{29}{28}y_{n+2} - \frac{1}{28}y_n. \tag{14}$$

CASE k = 5: Letting, v = u = 3 and equation (10) becomes:

$$y(x) = \alpha_0(x)y_n + \alpha_1(x)y_{n+1} + \alpha_2(x)y_{n+2} + h_n[\beta_2(x)f_{n+2} + \beta_3(x)f_{n+3}] + h_n^2\lambda_3(x)g_{n+3}. \tag{15}$$

In the same way, the continuous scheme is evaluated at $\eta = 5h_n$ and its first derivative at $\eta = (0, h_n, 3h_n, 5h_n)$ to have the following five discrete schemes.

$$y_{n+1} = \frac{6}{17}h_n^2g_{n+3} - \frac{36}{17}h_nf_{n+4} - \frac{28}{17}h_nf_{n+3} - \frac{6}{17}h_nf_{n+1} - \frac{1}{17}y_{n+4} + \frac{163}{51}y_{n+3} - \frac{36}{17}y_{n+2} - \frac{1}{51}y_n,$$

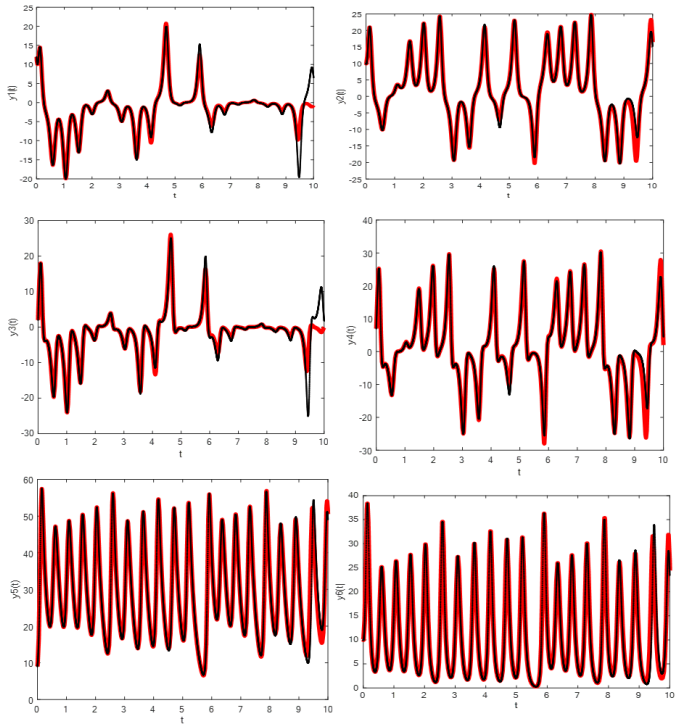

Figure 2. Comparison of the phase space between the SDETR$_2$s blended with GBDF for k=3 with $h = 10^{-1}$ to 10^{-5} and ODE 45 for Problem 1.

$$y_{n+2} = \frac{187}{906}h_n^2 g_{n+3} + \frac{1}{906}h_n^2 g_{n+2} - \frac{793}{1359}h_n f_{n+3} - \frac{197}{453}h_n f_{n+2} - \frac{157}{1812}y_{n+4} + \frac{18589}{16308}y_{n+3} - \frac{101}{1812}y_{n+1} + \frac{41}{16308}y_n,$$

$$y_{n+3} = -\frac{6}{49}h_n^2 g_{n+3} + \frac{26}{49}h_n f_{n+4} + \frac{27}{49}h_n f_{n+3} - \frac{1}{98}h_n f_n + \frac{9}{392}y_{n+4} + \frac{81}{98}y_{n+2} + \frac{9}{49}y_{n+1} - \frac{13}{392}y_n,$$

$$y_{n+4} = \frac{48}{55}h_n^2 g_{n+3} + \frac{12}{55}h_n f_{n+4} - \frac{16}{11}h_n f_{n+3} - \frac{72}{55}h_n f_{n+2} + \frac{728}{165}y_{n+3} - \frac{36}{11}y_{n+2} - \frac{8}{55}y_{n+1} - \frac{1}{165}y_n,$$

$$y_{n+5} = -60h_n^2 g_{n+3} + 160h_n f_{n+3} + 120h_n f_{n+2} + 30y_{n+4} - \frac{970}{3}y_{n+3} + 280y_{n+2} - 15y_{n+1} - \frac{2}{3}y_n. \quad (16)$$

3. CONVERGENCE ANALYSIS

In this section, the order, error constants, consistency and zero stability of the derived discrete schemes will be analyzed.

3.1. ORDER AND ERROR CONSTANT

The order and error constant of the discrete schemes in equation(14) and (16) are obtained or carried out in block form. Following Ref. [8] and Ref. [9], the local truncation error associated with the k-step second derivative multistep method (Equation 2) is the linear difference operator L defined as:

$$L[y(x) : h] = \sum_{i=0}^{k=0}\{\alpha_j y(x + jh_n) - h_n\beta_j y'(x + jh_n) - h_n^2\beta_j y'(x + jh_n)\}, \quad (17)$$

where y(x) is an arbitrary function, continuously differentiable on [a, b]. Expanding $y(x + jh_n)$ and its derivative $y'(x + jh_n)$ as Taylor series about x, and collecting terms in equation (17) give;

$$L[y(x) : h_n] = C_0 Z(x) + C_1 h_n Z^1(x) + ... + C_q h_n Z^q(x) + ..., (18)$$

where the constant C_q, q=0, 1, … are given as:

$$\begin{aligned} C_0 &= \textstyle\sum_{j=0}^{k} \alpha_j \\ C_1 &= \textstyle\sum_{j=0}^{k} j\alpha_j - \sum_{j=0}^{k} \beta_j \\ C_2 &= \tfrac{1}{2}\textstyle\sum_{j=0}^{k} j\alpha_j - \sum_{j=0}^{k} j\beta_j - \sum_{j=0}^{k} \lambda_j \\ &\vdots \\ C_q &= \tfrac{1}{q}\textstyle\sum_{j=0}^{k} j^q\alpha_j - \frac{1}{(q-1)!}\sum_{j=0}^{k} j^{q-1}\beta_j - \frac{1}{(q-2)!}\sum_{j=0}^{k} j^{q-2}\lambda_j, q = 3, 4, ... \\ &\vdots \end{aligned} \quad (19)$$

The method in equation (14) expressed in the form of equation (17) produces the values of the continuous coefficients of the method as:

$$\alpha_0 = \left(\frac{1}{28}, -\frac{7}{23}, \frac{1}{2}\right), \alpha_1 = \left(1, -\frac{16}{23}, 15\right), \alpha_2 = \left(-\frac{29}{28}, 1, -\frac{33}{2}\right),$$
$$\alpha_3 = (0, 0, 1), \beta_0 = \left(0, \frac{2}{23}, 0\right), \beta_1 = \left(-\frac{23}{56}, \frac{16}{23}, -6\right),$$
$$\beta_2 = \left(-\frac{9}{14}, \frac{12}{23}, -9\right), \beta_3 = \left(-\frac{1}{56}, 0, 0\right), \lambda_2 = \left(\frac{5}{28}, -\frac{2}{23}, 3\right). \quad (20)$$

Substituting these values of the continuous coefficients in equation (20) into equation (19), we have:

$$
\begin{aligned}
C_0 &= \alpha_0+\alpha_1+\alpha_2+\alpha_3 = \begin{bmatrix}0\\0\\0\end{bmatrix}\\
C_2 &= \tfrac{1}{2}(\alpha_0+\alpha_1+\alpha_2+\alpha_3)-(\beta_0+\beta_1+\beta_2+\beta_3) = \begin{bmatrix}0\\0\\0\end{bmatrix}\\
C_1 &= (\alpha_0+\alpha_1+2\alpha_2+3\alpha_3)-(\beta_0+\beta_1+\beta_2+\beta_3) = \begin{bmatrix}0\\0\\0\end{bmatrix}\\
C_3 &= \tfrac{1}{6}(\alpha_1+2^3\alpha_2+3^3\alpha_3)-\\
&\qquad \tfrac{1}{2}(\beta_1+2^2\beta_2+3^2\beta_3)-(\lambda) = \begin{bmatrix}0\\0\\0\end{bmatrix}\\
C_3 &= \tfrac{1}{6}(\alpha_1+2^3\alpha_2+3^3\alpha_3)-\\
&\qquad \tfrac{1}{2}(\beta_1+2^2\beta_2+3^2\beta_3)-(\lambda_2) = \begin{bmatrix}0\\0\\0\end{bmatrix}\\
C_4 &= \tfrac{1}{24}(\alpha_1+2^4\alpha_2+3^4\alpha_3)-\tfrac{1}{6}(\beta_1+2^3\beta_2+3^3\beta_3)-\\
&\qquad \tfrac{1}{2}(2^2\lambda_2) = \begin{bmatrix}0\\0\\0\end{bmatrix}\\
C_5 &= \tfrac{1}{120}(\alpha_1+2^5\alpha_2+3^5\alpha_3)-\tfrac{1}{24}(\beta_1+2^4\beta_2+3^4\beta_3)-\\
&\qquad \tfrac{1}{6}(2^3\lambda_2) = \begin{bmatrix}0\\0\\0\end{bmatrix}\\
C_6 &= \tfrac{1}{720}(\alpha_1+2^6\alpha_2+3^6\alpha_3)-\\
&\qquad \tfrac{1}{120}(\beta_1+2^5\beta_2+3^5\beta_3)-\tfrac{1}{24}(2^4\lambda_2) = \begin{bmatrix}\frac{13}{10080}\\ \frac{1}{1035}\\ \frac{1}{60}\end{bmatrix},
\end{aligned}
\tag{21}
$$

solving gives equation (21) $C_0 = C_1 = C_2 = C_3 = C_4 = C_4 = 0$ but $C_6 \neq 0$ that is $C_{p+2} \neq 0$ which is the error constant of the method and $C_{p+2}h^{p+2}y^{p+2}(x_n)$ is the principal local truncation error at the point x_n. Thus the local truncation error (LTE) of the method is written as:

$$LTE = C_{p+2}h^{p+2}y^{p+2}(x_n) + O(h^{p+3}). \tag{22}$$

Using equation (17) – (20), method equation (14) is of uniform order [5, 5, 5] ^{T} and with the following error constant $\left[\frac{13}{10080}, \frac{1}{1035}, \frac{1}{60}\right]^T$. Similarly, the order and error constant of the block method equation (16) is carried out following the same producer as in case k=3. Therefore, equation (16) is of order p = 7 and error constant $\left[\frac{1}{4760}, -\frac{31}{217440}, -\frac{3}{27440}, -\frac{1}{3850}, \frac{1}{28}\right]^T$.

3.2. CONSISTENCY

All the methods in equation (14) and (16) have their orders greater than one, so as in Ref. [10], the methods are consistent.

3.3. ZERO STABILITY

The zero stability of the discrete schemes in Eq. (14) is determined in block forms using the approach in Ref. [9]. The method Eq. (14) is represented as a single block r-point multistep method of the form:

$$\theta^{(1)}Y_{u+1} = \theta^{(0)}Y_u + h_u\delta^{(1)}F_u + h_u^2\tau^{(1)}G_u,$$

where,

$$
\begin{aligned}
Y_{u+1} &= (y_{n+1}, y_{n+2}, y_{n+3})^T,\\
Y_u &= (y_{n-3}, y_{n-2}, y_{n-1})^T,\\
F_{u+1} &= (f_{n+1}, f_{n+2}, f_{n+3})^T,\\
G_{u+1} &= (g_{n+1}, g_{n+2}, g_{n+3})^T,
\end{aligned}
\tag{23}
$$

for u=0, … and n=0, 1, 2, 3, …, N-3, and the matrices $\theta^{(1)}, \delta^{(1)}, \tau^{(1)}$ are 3 by 3 matrices whose entries are given by the coefficients of Eq. (16).

3.4. DEFINITION (ZERO STABILITY)

A block LMM is said to be zero stable provided the roots $R_{i,j}$, i, j=1,...,k of the first characteristic polynomial ρ (R):

$$\rho(R) = \det\left[\sum_{j=0}^{k} A^{(j)}R^{k-1}\right] = 0, \tag{24}$$

satisfy $|R| \leq 1$, and for those roots with $|R| = 1$, the multiplicity does not exceed two.

The block method Eq. (14) written in the form of Eq. (24) gives the characteristic polynomial of the method as:

$$
\begin{aligned}
&\rho(R) = (R^2 - R)R = (R^3 - R^2)\\
&R(R^2 - R) = 0,
\end{aligned}
$$

which implies,

$$R_1 = 1, R_2 = R_3 = 0.$$

Therefore, the block method in Eq. (14) in Eq. (24) and hence is zero stable in Ref. [10]. Following the procedure as in Eq. (14), we determined the zero stability of the block method Eq. (16). Also, is zero-stable in Ref. [10].

3.5. CONVERGENCE ANALYSIS

The block methods Eq. (14) and Eq. (16) are all convergent in Ref. [10], since they are both consistent and zero-stable.

3.6. STABILITY ANALYSIS

In this section, the stability of the derived methods in Eq. (14) and Eq. (16) are investigated as:

$$
\begin{vmatrix} 1 & -\frac{29}{28} & 0\\ -\frac{16}{23} & 1 & 0\\ 15 & -\frac{33}{2} & 1\end{vmatrix}\begin{vmatrix} y_{n+1}\\ y_{n+2}\\ y_{n+3}\end{vmatrix} = \begin{vmatrix} 0 & 0 & -\frac{1}{28}\\ 0 & 0 & \frac{7}{23}\\ 0 & 0 & -\frac{1}{2}\end{vmatrix}\begin{vmatrix} y_{n-2}\\ y_{n-1}\\ y_n\end{vmatrix} +
h\begin{vmatrix} -\frac{23}{56} & -\frac{9}{14} & -\frac{1}{56}\\ -\frac{16}{23} & \frac{12}{23} & 0\\ -6 & -9 & 0\end{vmatrix}\begin{vmatrix} f_{n+1}\\ f_{n+2}\\ f_{n+3}\end{vmatrix} + h\begin{vmatrix} 0 & 0 & 0\\ 0 & 0 & \frac{2}{23}\\ 0 & 0 & 0\end{vmatrix}\begin{vmatrix} f_{n-2}\\ f_{n-1}\\ f_n\end{vmatrix} +
h_n^2\begin{vmatrix} 0 & \frac{5}{28} & 0\\ 0 & -\frac{2}{23} & 0\\ 0 & 3 & 0\end{vmatrix}\begin{vmatrix} g_{n+1}\\ g_{n+2}\\ g_{n+3}\end{vmatrix} + h_n^2\begin{vmatrix} 0 & 0 & 0\\ 0 & 0 & 0\\ 0 & 0 & 0\end{vmatrix}\begin{vmatrix} g_{n-2}\\ g_{n-1}\\ g_n\end{vmatrix},
$$

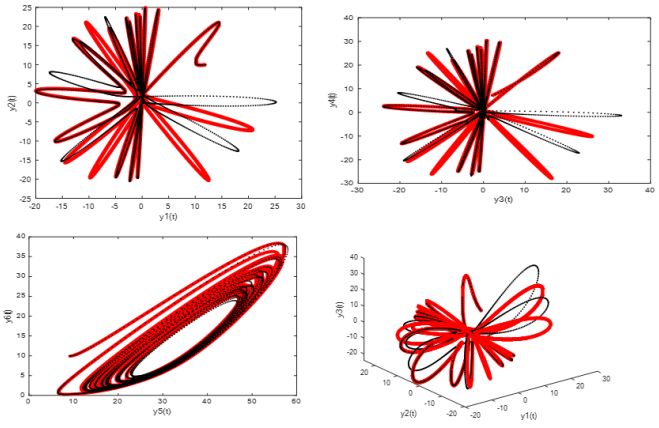

Figure 3. Comparison of phase portraits for problem 1 between SDETR$_2$s blended with GBDF for k=3 with $h = 10^{-1} to 10^{-5}$and ODE 45.

where,

$$\Psi = \begin{vmatrix} 1 & -\frac{29}{28} & 0 \\ -\frac{16}{23} & 1 & 0 \\ 15 & -\frac{33}{2} & 1 \end{vmatrix},$$

$$\Phi = \begin{vmatrix} 0 & 0 & -\frac{1}{28} \\ 0 & 0 & \frac{7}{23} \\ 0 & 0 & -\frac{1}{2} \end{vmatrix},$$

$$\Sigma = \begin{vmatrix} -\frac{23}{56} & -\frac{9}{14} & -\frac{1}{56} \\ -\frac{16}{23} & \frac{12}{23} & 0 \\ -6 & -9 & 0 \end{vmatrix},$$

$$\Omega = \begin{vmatrix} 0 & 0 & 0 \\ 0 & 0 & \frac{2}{23} \\ 0 & 0 & 0 \end{vmatrix},$$

$$\Gamma = \begin{vmatrix} 0 & \frac{5}{28} & 0 \\ 0 & -\frac{2}{23} & 0 \\ 0 & 3 & 0 \end{vmatrix},$$

$$\Pi = \begin{vmatrix} 0 & 0 & 0 \\ 0 & 0 & 0 \\ 0 & 0 & 0 \end{vmatrix}$$

The elements of the matrices $\Psi, \Phi, \Sigma, \Gamma, \Omega, \Pi$, are substituted into the characteristic equation of Eq. (25) in Maple Software.

$$N(\gamma) = \det\left|\gamma(\Psi - \Sigma\chi - \Gamma\chi^2) - \Phi - \Omega\chi - \Pi\chi^2\right| = 0, \quad (25)$$

$$\det\begin{bmatrix} \gamma(1+\frac{23}{56}\chi) & \gamma(-\frac{29}{28}+\frac{9}{14}\chi-\frac{5}{28}\chi^2) & \frac{1}{56}\gamma\chi+\frac{1}{28} \\ \gamma(-\frac{16}{23}-\frac{16}{23}\chi) & \gamma(1-\frac{12}{23}\chi+\frac{2}{23}\chi^2) & -\frac{7}{23}-\frac{2}{23}\chi \\ \gamma(15+6\chi) & \gamma(-\frac{33}{2}+9\chi-3\chi^2) & \gamma+\frac{1}{2}\chi \end{bmatrix} = 0.$$

Solving, we obtain the stability polynomial,

$$N(\gamma) = -\frac{45}{161}\gamma^2 - \frac{9}{23}\gamma^2\chi - \frac{153}{644}\gamma^2\chi^2 - \frac{51}{644}\gamma^3\chi^2 - \frac{72}{161}\gamma^3\chi + \frac{9}{28}\gamma^3\chi^2 - \frac{9}{644}\gamma^4\chi^4 + \frac{9}{322}\gamma^3\chi^4 + \frac{45}{161}\gamma^3. \quad (26)$$

Differentiating Eq. (26) with respect to χ we obtain the derivative as:

$$N(\gamma) = -\frac{9}{23}\gamma^2 - \frac{153}{322}\gamma^2\chi - \frac{153}{644}\gamma^2\chi^2 - \frac{72}{161}\gamma^3 + \frac{9}{14}\gamma^3\chi - \frac{9}{23}\gamma^3\chi^2 - \frac{9}{161}\gamma^2\chi^3 + \frac{18}{161}\gamma^3\chi^3. \quad (27)$$

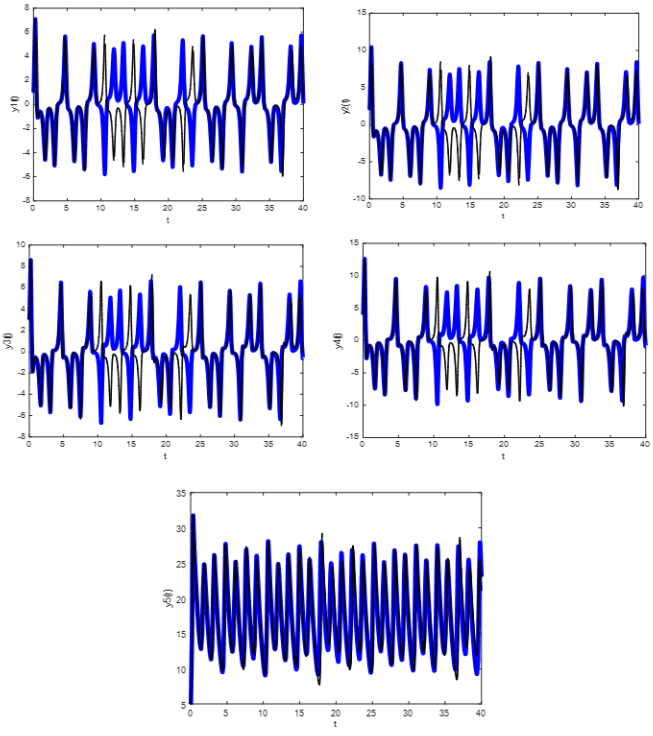

Figure 4. Comparison of phase space between the SDETR$_2$s blended with GBDF blue line with$h = 10^{-1} to 10^{-5}$and ODE 45 black line for Problem 2.

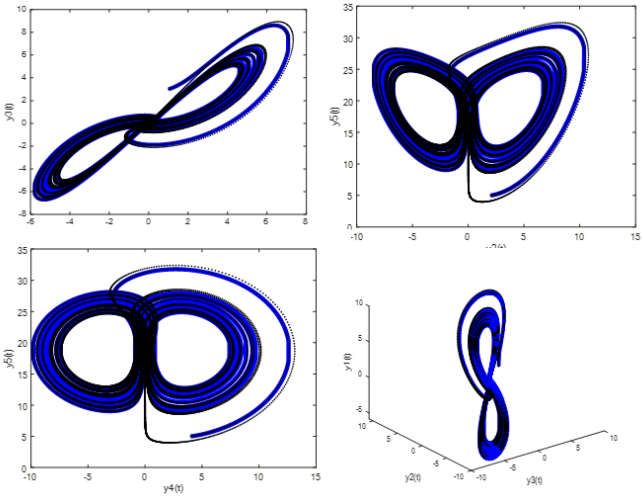

Figure 5. Comparison of phase portraits for problem 2 between SDETR$_2$s blended with GBDF for k=5 blue line with $h = 10^{-1} to 10^{-5}$and ODE 45 black line.

Then, Eq. (27) is substituted into MATLAB code to plot the regions of absolute stability for methods Eq. (14) and Eq. (16) are shown in Figure 1.

4. IMPLEMENTATION

4.1. NUMERICAL EXAMPLES

In this section, some real-life problems with complex hyperchaotic behaviours are solved numerically using our new meth-

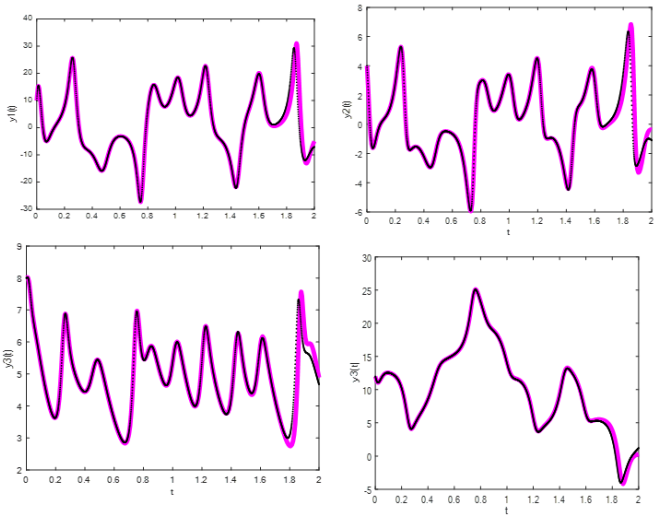

Figure 6. Comparison of phase space of Problem 3 between SDETR$_2$s blended with GBDF for k=3 Magenta line and $h = 10^{-1} to 10^{-5}$ and ODE 45 black line.

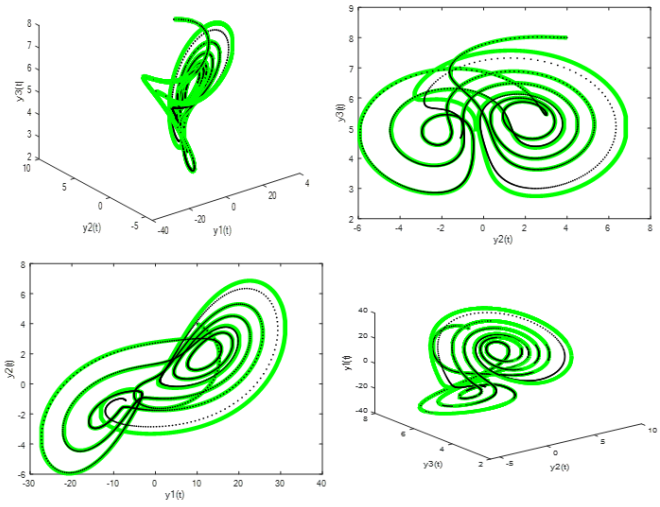

Figure 7. Comparison of phase portraits of Problem 3 between SDETR$_2$s blended with GBDF for k=5 with $h = 10^{-1} to 10^{-5}$and ODE 45.

ods and results compared with those obtained from existing method in literature and the Matlab ODEs solvers. We considered the following problems in Refs. [11–13].

4.1.1. Example 1: Hyperchaotic Lorenz system

The hyperchaotic complex Lorenz system was derived in Ref. [11] when modeling two-dimensional fluid cell between two parallel plates at different temperatures.

$$\begin{aligned} y_1' &= a(y_3 - y_1) \\ y_2' &= a(y_4 - y_2) + y_6 \\ y_3' &= by_1 - y_3 - y_1y_5 \\ y_4' &= by_2 - y_4 - y_2y_5 + y_6 \\ y_5' &= -y_1y_3 + y_2y_4 - cy_5 \\ y_6' &= y_1y_3 + y_2y_4 - dy_6, \end{aligned}$$

where, a=15, b=36, c=4.5, d=12, $y_1(0)$=12, $y_2(0)$=10, $y_3(0)$=2, $y_4(0)$=7, $y_5(0)$=9, $y_6(0)$=10, for t ∈ [0, 10] and h=10^{-1} to 10^{-5}.

4.1.2. Example 2: Hyperchaotic Permanent Magnet Synchronous

State equations of hyperchaotic permanent magnet synchronous motor system in a field-oriented motor can be described by the following system in Ref. [12]:

$$\begin{aligned} y_1' &= a(y_3 - y_1) \\ y_2' &= a(y_4 - y_2) \\ y_3' &= by_1 - y_3 - y_1y_5 \\ y_4' &= by_2 - y_4 - y_2y_5 \\ y_5' &= y_1y_3 + y_2y_4 - y_5, \end{aligned}$$

where, a=11, b=20, $y_1(0)$=1,$y_2(0)$=2, $y_3(0)$=3, $y_4(0)$=4, $y_2(0)$=5 for t∈ [0, 40] and h=10^{-1} to 10^{-5}.

4.1.3. Example 3: Hyperchaotic Qi system

We consider the hyperchaotic Qi dynamics in Ref. [13] described by:

$$\begin{aligned} y_1' &= a(y_2 - y_1) + \psi y_2y_3 \\ y_2' &= cy_1 - dy_1y_3 + y_2 + y_4 \\ y_3' &= y_1y_2 - by_3 \\ y_4' &= -\varphi y_2, \end{aligned}$$

where, a=35, b=4.9, c=25, d=5, ψ=35, φ=22, $y_1(0)$=10, $y_2(0)$=4, $y_3(0)$=8, $y_4(0)$=12, for t ∈ [0, 10] and h=10^{-1} to 10^{-5}.

4.2. RESULTS

4.3. RESULTS AND DISCUSSIONS

In this section, we present the results for the regions plotted and numerical results of our new methods SDETR$_2$s with GBDF for k = 3 and 5, to solve three hyperchaotic problems. From Figure 1, the regions are all A-stable, hence, the methods are suitable for solving hyperchaotic ODEs. The value of h was varied between 0.1 and 0.00001 in Ref. [10] and 0.1 and 0.0001 in Refs. [11, 13]. The accuracy level used in this work is six decimal places. The results of our newly derived method are compared with existing method in literature and MATLAB in-built solvers for IVPs of ODEs; in particular, the routine ODE 45 was used. By existence and uniqueness theorem 1, trajectories cannot merge or cross, the strange attractors are all unique. The entire phase space and phase portrait are in agreement with each other.

5. CONCLUSION

In this work, we have constructed SDETR$_2$s blended with GBDF for k = 3 and k = 5 with variable step size for solving nonlinear IVPs of ODEs with hyperchaotic properties. The methods derived are convergent and A-stable. The new block methods are self-starting, hence eliminating the use of starting values. From the result of the numerical simulations carried out in Refs. [10, 12, 13], the methods are efficient and attractive for solving hyperchaotic, other nonlinear and linear ODEs as displaced by

numerical results in the tables, time series and phase portrait solution curves compared with MATLAB ODEs in-built in solver. The step size was varied to overcome the claim in Ref. [14].

Table 1 presents a comparison between the SDETR$_2$s with GBDF and the MSRM for Problem 1 at selected values of time points (t). Figures 2 and 3 display the corresponding time series (phase space) graphs and phase portraits, which demonstrate a strong agreement between the SDETR$_2$s with GBDF for k=3 and ODE 45.

Table 2 compares the numerical results of our new method with those of ODE 45 for the problem 2, revealing good agreement between the two methods as time (t) progresses. Figure 4 compares the SDETR$_2$s with GBDF for k=3 and ODE 45 time series for Problem 2, exhibiting good agreement. Figure 5 displays the corresponding phase portraits, which demonstrate identical results from numerical simulations using our new method and the ODE solver.

Table 3 presents a comparison between the results of our new method and ODE 45 for all the dependent variables of the Qi-system at selected time values (t). The good agreement between the SDETR$_2$s with GBDF and ODE 45 solver results, as seen in Figures 6 and 7, confirms the validity of the proposed new scheme approach for solving nonlinear and hyperchaotic systems. The time series plots and phase portraits for the Qi-system shown in these Figure demonstrate the accuracy of the SDETR$_2$s with GBDF for k=3 and ODE 45 method compared to other methods.

ACKNOWLEDGMENT

We wish to acknowledge God for all his inspirations and Late Oche Felix.

References

[1] O. E. Rössler, ‘‘An equation for continuous chaos’’, Physics Letters **57** (1976) 397. http://dx.doi.org/10.1016/0375-9601(76)90101-8.

[2] S. S. Motsa, P. Dlamini & M. Khumalo, ‘‘A new multistage spectral relaxation method for solving chaotic initial value systems’’, Nonlinear Dynamic **72** (2012) 265. https://doi.org/10.1007/s11071-012-0712-8.

[3] S. Motsa, ‘‘A new piecewise-quasi linearization method for solving chaotic systems of initial value problems’’, Central European Journal of Physics **10** (2012) 936. https://doi.10.2478/s11534-011-0124-2.

[4] S. S. Motsa, Y. Khan & S. Shateyi, ‘‘Application of piecewise successive linearization method for the solutions of the Chen chaotic system’’, Journal of Applied Mathematics **2012** (2012) 258948. https://doi.org/10.1155/2012/258948.

[5] H. M. Nour, A. Elsaid & A. Elsonbaty, ‘‘Comparing the multistage and PADE techniques for iterative methods in solving nonlinear food chain model’’, Mathematics and Computer Science **2** (2012) 810. https://scik.org/index.php/jmcs/article/view/163/0.

[6] P. Onumanyi, U. W. Sirisena & S. N. Jator, ‘‘Continuous finite difference approximations for solving differential equations’’, International Journal of Computer Mathematics **72** (1999) 15. https://dx.doi.org/10.1080/00207169908804831.

[7] L. Brugnano & D. Trigiante, *Solving differential problems by multistep initial and boundary value methods*, Gordon and Breach Science Publishers, Amsterdam, Netherlands, 1998, pp. 153–154. https://api.semanticscholar.org/CorpusID:118368291.

[8] S. O. Fatunal, ‘‘Block Method for second order differential equations’’, International Journal of Computer Mathematics **41** (1991) 55. https://dx.doi.org/10.1080/00207169108804026.

[9] J. D. Lambert, *Computational methods in ordinary differential equations*, John Willey and Sons, New York, USA, 1973, pp. 523-523. https://doi.org/10.1002/zamm.19740540726.

[10] S. O. Fatunla, ‘‘Numerical integrators for stiff and highly oscillatory differential equations’’, Journal of Mathematical Computation **34** (1980) 373. https://doi.org/10.2307/2006091.

[11] J. Yu, B. Chen, H. Yu & J. Gao, ‘‘Adaptive fuzzy tracking control for the chaotic permanent magnet synchronous motor derive system via backstepping’’, Nonlinear Analysis: Real World Applications **34** (2011) 671. http://doi.org/10.1016/j.nonrwa.2010.07.009.

[12] F. Zhang, C. Mu, X. Wang, I. Ahmed & Y. Shu, ‘‘Solution bounds of a new complex PMSM system’’, Nonlinear Dynamics **74** (2013) 1041. http://dx.doi.org/10.1007/s11071-013-1022-5.

[13] Z. Chen, Y. Yang, G. QI & Z. Yuan, ‘‘A novel by hyperchaos system only with one equilibrium’’, Physics Letters A **360** (2007) 696. https://doi.org/10.1016/j.physleta.2006.08.085.

[14] L. S. Yao, ‘‘Computed chaos or numerical errors’’, Nonlinear Analysis Modelling and Control **15** (2010) 109. https://doi.org/10.15388/NA.2010.15.1.14368.